Conformational Characteristics of Polymethylene Chains in Melts and in Various Phantom Chains from Explicit Atom Molecular Dynamics Simulations

Jie Han and Richard L. Jaffe

NASA Ames Research Center, Moffett Field, California 94035

Do Y. Yoon*

IBM Almaden Research Center, San Jose, California 95120-6099

Received December 3, 1996; Revised Manuscript Received May 19, 1997[⊗]

ABSTRACT: Conformer populations, mean-square chain dimensions, and end-to-end distance distributions for polymethylene (PM) chains, $H(CH_2)_nH$ with $n = 13$, 44, and 100, in melts and in various phantom chains have been studied using a parallel computational method of molecular (and Brownian) dynamics simulations with a well-calibrated explicit atom force field. The specific volume−temperature properties of the simulated melt systems are in excellent agreement with experiments. Conformational characteristics of PM chains in melts are identical to those of 1,5 phantom chains, characterized by short-range intramolecular interactions between the atoms separated by up to four skeletal bonds, which correspond to unperturbed chains in Θ solvents according to recent implicit solvent model results of Sariban et al. and Destrée et al. Moreover, a Gaussian approximation of end-to-end distance distributions is found to be valid only for long PM chains with *n* greater than 100. According to our simulation results, the characteristic ratio C_∞ for unperturbed polyethylene chains is found to be ca. 7.9 at 413 K. This value is larger than the generally accepted value, 6.8 (derived from intrinsic viscosity data for relatively polydisperse polyethylene samples), but is corroborated by recent small angle neutron scattering results (7.8 ± 0.4) for melt chains of nearly monodisperse samples. The fact that PM chains exhibit identical conformational characteristics in melts, 1,5 phantom chains, and Θ solvents is attributed to the lack of any correlation between local chain conformations and (polymer−polymer or polymer−solvent) intermolecular attractions. Departures from such an ideal behavior seen for other polymers are also discussed.

Introduction

The current understanding of polymer chains in bulk amorphous states is based on the fundamental proposition that the conformational characteristics of melt chains are identical to those of unperturbed chains in Θ solvents, for which the effects of long-range excluded volume interactions are completely absent, as first proposed by Flory.[1] The unperturbed chains thus defined are completely dependent upon short-range intramolecular interactions, which are normally approximated by truncating them beyond a certain range, for example, beyond 1,5 interactions between atoms separated by four skeletal bonds (dependent on two consecutive skeletal torsional angles) in polymethylenes. Consideration of such (approximated) short-range interactions has been further simplified by describing them by rotational isomeric state (RIS) models, which replace continuous torsional distributions with a set of discrete, suitably chosen, isomeric torsional states.[2−4] The RIS models usually contain a number of geometric and energetic parameters which are determined directly from experiments or indirectly from fits of experimental results for conformation-dependent properties such as unperturbed chain dimensions, mean-square dipole moments, NMR vicinal couplings, etc. Therefore, conformational characteristics of melt chains of varying chemical structures have been traditionally described in terms of appropriate RIS models, together with their geometric and energetic parameters.

The advancement of molecular simulations, via Monte Carlo (MC) and molecular dynamics (MD) methods, allows the determination of conformational properties of polymers in terms of realistic distributions of torsional angles and skeletal bond angles without the restrictive approximations of RIS models. Moreover, one can now accurately determine the characteristics of unperturbed chains without making *a priori* approximations on what constitutes the short-range interactions. Most importantly, the conformational characteristics of melt chains can be investigated and compared directly with those of unperturbed chains in order to test the accuracy of Flory's proposition.

Recently, these molecular simulation methods have been employed to study polymethylene chains (PM),[5−9] an important prototype of flexible polymers. For example, using an implicit solvent model that scales the attractive part of interatomic interactions appropriately, Sariban, Brickmann, van Ruiten and Meier (SBRM),[5] and Destrée, Lyulin and Ryekaert (DLR)[6] simulated the unperturbed polymethylene chains under the ideal condition which yields the mean-square end-to-end distance $\langle r^2 \rangle$ to be linearly proportional to the number of skeletal bonds. According to SBRM,[5] the unperturbed PM chains correspond to 1,6 phantom chains (m=5 in the notation of reference 5) which include intramolecular interactions up to 1,6 interactions, i.e., interactions between the atoms separated by five skeletal bonds, depending on three consecutive torsions. This finding is contrary to the generally accepted idea that the second-order RIS model (including up to 1,5 interactions) is a good representation of unperturbed PM chains.[2−4,10,11] (SBRM found that the value of $\langle r^2 \rangle$ for 1,6 phantom chains is considerably (by ca. 7%) smaller than that for 1,5 phantom chains.) Moreover, according to DLR,[6] the characteristic ratio $C_\infty = \langle r^2 \rangle_0 / n' l^2$ at high molecular weights ($\langle r^2 \rangle_0$ being the mean-square end-to-end distance of unperturbed chains, n' the number of

[⊗] Abstract published in *Advance ACS Abstracts,* September 15, 1997.

S0024-9297(96)01772-X CCC: $14.00

skeletal bonds, and l the C−C bond length) was found to be 7.9 ± 0.2 at 400 K. This is considerably larger than the value of 6.8 predicted by the well-established RIS model and is generally believed to be in agreement with experiments.[4,11] The discrepancy was attributed to the deficiency of the united atom (UA) force field used.[6] Alternatively, Baschnagel, Quin, Paul, and Binder (BQPB)[7] suggested that the experimental results could be reconciled by the phantom chains containing up to 1,8 intramolecular interactions.

Other workers have used molecular simulations to make a direct comparison between melt chains and phantom chains. Pant and Theodorou (PT) compared intramolecular pair density functions of melt chains and 1,5 (second-order) phantom chains using MC methods.[8] They found that intrachain structures in these two states were identical for PM chains of $n = 23$ and $n = 78$, but no comparisons were made for conformer populations and chain dimensions. Brown, Clarke, Okuda, and Yamazaki (BCOY)[9] recently showed that conformational characteristics of PM chains with $n \leq 100$ in melts are very close to those of 1,5 phantom chains. However, their predicted value of C_∞ (∼10) is too large. Moreover, considering the conclusion of SBRM that 1,5 phantom chains are more extended than the unperturbed chains, the finding of BCOY appears to contradict Flory's proposition.

Therefore, even for PM chains, the simplest model polymer, there exist no clear answers on the following three important questions: (i) What are the characteristics of unperturbed PM chains? (ii) What are the relevant short-range interactions one should consider in an appropriate RIS model (second-order or a higher order)? (iii) How closely do conformational characteristics of PM chains in melts match those of unperturbed chains? These questions, left unanswered by previous molecular simulations, cannot be resolved satisfactorily by available experiments either, since according to a very recent work by Zirkel et al. the commonly used method of determining unperturbed chain statistics from intrinsic viscosity experiments is open to serious question.[12] The only recourse is to carefully carry out molecular simulations which accurately take into account all the relevant interactions in melts as well as in isolated chains.

In this regard, it should be noted that the previous simulation results discussed above are all based on the united atom (UA) approximation which collapses the hydrogens of PM chains onto the skeletal carbon atoms. The ability of UA force fields in general to accurately describe short-range intramolecular interactions of unperturbed chains is open to question. Furthermore, the UA force fields used by PT[8] and BCOY[9] are truncated at too short interatomic distances (ca. 4.5 Å), corresponding to the minimum in pairwise interactions. It is therefore questionable whether the short-range interactions that characterize unperturbed chains are fully accounted for by their 1,5 phantom chains.

Recently, in order to overcome the shortcomings of UA models,[13,14] explicit atom (EA) force fields for PM chains were developed[15,16] which yielded a good agreement between the simulation results and experiments for many equilibrium and dynamic properties of PM melts, such as X-ray scattering functions and pressure−volume−temperature (PVT) properties,[16,17] ^{13}C NMR spin−lattice relaxation times,[16,17] and molecular diffusion coefficients.[18] Although a detailed comparison was not made between the conformational properties of unperturbed PM chains and melt chains, some interesting observations of conformational features were made from simulations of n-$C_{44}H_{90}$ melts. It was seen that chain dimensions of melt chains obtained from simulations with EA force fields are larger than the values predicted by the previous RIS model[17] and that the monomer friction factors of melt chains from simulations show deviations from the Rouse model predictions.[18] It is puzzling why the EA simulations are so successful in reproducing many other properties of PM chains[15−18] but fail to reproduce the characteristic ratio predicted by the RIS model, which was carefully parametrized to match chain dimensions and temperature coefficients derived from intrinsic viscosity experiments. The problem with monomer friction factors was postulated to arise from deviation from the Gaussian distribution of end-to-end chain vectors, based on previous RIS model calculations,[19] but no result was presented for the distribution of chain vectors from force field based molecular simulations.

The present work presents conformational characteristics of PM chains, obtained from molecular dynamics simulations using a well-calibrated EA force field, focusing on the following three aspects. First, we compare conformational properties of melt chains with those of phantom chains with varying intramolecular cutoff segment lengths and also with those of unperturbed chains derived from the phantom chain simulations. Second, we determine in detail the distribution of chain end-to-end distances, $w(r)$, and its approach to a Gaussian distribution as the chain length increases. Third, on the basis of our simulation results and recent small angle neutron scattering experiments on nearly monodisperse samples,[20] we discuss a new value for the characteristic ratio C_∞ of unperturbed PM chains in the long chain limit, which is considerably greater than the generally accepted value of 6.8 at 413 K.

Simulation Details

Simulation systems are comprised of N polymethylene chains, $H(CH_2)_nH$, with $n = 13$, 44, and 100, and the number of chains, $N = 100$, 45, and 64, respectively. They are represented by explicit C and H atoms, with total atom numbers of 4100, 6030, and 19328 for these three systems. Most of the simulations have been carried out by using parallel molecular dynamics (MD) or Brownian dynamics (BD) algorithms in order to obtain trajectories long enough to sample sufficient chain configurations. The bond lengths were allowed to vary in parallel computations (for optimum efficiency as discussed below) while they were constrained using the SHAKE algorithm in serial computations, as described in the previous work.[16−18] No noticeable differences in conformational properties and PVT properties are found between the constrained and unconstrained bond-length treatments. The EA force field is taken from the previous work.[15,16] The bond stretch constant adopted here, 634 kcal Å^{-2}/mol for both the C−C bond and the C−H bond, is taken from ref 15. Nonbonded interactions were truncated at 9 Å in order to fully take into account the attractive interactions for isolated phantom chains. The cutoff was 6 Å for the melt chains since previous work showed no difference between the cutoff of 6 Å and that of 10 Å for melt PM chains.[16] Table 1 lists the force field parameters for bonded and nonbonded interactions, which include correction of some typographic errors in the nonbonded EA force field parameters in ref 16. No partial charges or electrostatic terms are included in this force field.

Table 1. Force Fields in Polymethylene Simulation[a]

stretch	$u = {}^1/_2 k_s(R - R_0)^2$			
	C−C	$k_s = 634$	$R_0 = 1.53$	
	C−H	634	1.09	
bending	$u = {}^1/_2 K_b(\theta - \theta_0)^2$			
	C−C−C	$k_\theta = 108$	$\theta_0 = 1.937$	
	C−C−H	86	1.911	
	H−C−H	77	1.883	
torsion	$u = {}^1/_2[k_{t1}(1 - \cos\phi) + k_{t3}(1 - \cos 3\phi)]$			
	C−C−C−C	$k_{t1} - 0.340$	$k_{t3} = 0.630$	
	H−C−C−X	0.000	0.234	
	X = C or H			
nonbonded	$u = a\exp(-bR) - c/R^6$			
EA	C, C	$a = 14969$	$b = 3.09$	$c = 639$
	C, H	4318	3.42	138
	H, H	2648	3.74	27.3

[a] Units: energy, kcal/mol; length, Å; angle, radians.

Nosé's constant temperature MD method[21] with a five-value predictor−corrector integration algorithm is used for melt simulations. The samples of $C_{44}H_{90}$ melts have been taken from the previous work,[18] in which ~2 ns constant temperature and constant volume (NVT) MD simulation was already performed for equilibration. In this work, these samples were further relaxed by a constant temperature and constant pressure (NPT) MD run of 200 ps at the desired temperature before conformational sampling was started. The $C_{13}H_{28}$ melts were prepared by *NPT* MD procedures starting from a very large periodic box in which the chains, in a very low concentration, adopt random initial configurations. The systems of $C_{13}H_{28}$ melts were investigated for conformational statistics after the energy and *PVT* properties had reached equilibrium values.

For simulations of isolated phantom chains, we used a constant temperature Brownian dynamics (BD) simulation method, in which no interchain interactions were included. It has been shown that the BD method is particularly appropriate to study the conformational behavior of polymer chains in solutions or phantom chain states.[22−24] The BD method in this work is similar to that used by Winkler, Matsuda, and Yoon[22] with a slightly different friction coefficient, γ ($1/\gamma = 1000$ and 10000 fs for C and H atoms, respectively, in place of the value of 748 fs for the CH_2 united atom). Well-relaxed melt samples were used as initial phantom chains in BD simulations of $C_{13}H_{28}$ and $C_{44}H_{90}$ chains. These samples were equilibrated by 500 ps BD runs without periodic boundary conditions and intermolecular interactions. The conformational sampling was then performed by additional BD simulation runs. For $C_{100}H_{202}$ chains, only 1,5 phantom chains were studied by BD simulations, with initial random configurations equilibrated for 200 ps before sampling runs.

Once block averages over MD time intervals (400 ps) remain constant for the temperature, the energies, and the conformational properties (conformer populations and mean-square chain dimensions) as well as the melt volume (in *NPT* MD runs), the system is considered to be equilibrated. Thus, the equilibrium conformational properties discussed in this paper are determined from block averages obtained for such equilibrated systems. The instantaneous properties always fluctuate around their average or equilibrium values, and a long trajectory is required to sample a sufficiently representative configurational space. In this work, the trajectory for sampling runs was 2 ns for melts and phantom chains of $C_{13}H_{28}$ and $C_{44}H_{90}$ and 10 ns for phantom chains of $C_{100}H_{202}$, with sampling interval of 0.5 ps. These sampling times were found to be sufficient to obtain time-independent block averages of chain dimensions. They are also longer than Rouse relaxation times of melt chains, a necessary condition for adequate conformational sampling as shown by the results of BCOY.[9] Statistical standard error in the present work is <1% for fractional conformer populations and <2% for chain dimensions, $\langle s^2 \rangle$.

The parallel computations were carried out on an IBM SP1/SP2 computer using a parallel MD/BD algorithm of atom decomposition with a massage passing interface (MPI) for communication.[25] In this algorithm, atoms in each molecule are distributed over 4 to 32 processors according to cyclic partitioning to achieve good load balance. For parallel MD simulations, the domain decomposition algorithm is very efficient if system size, L, and cutoff distance, R_c, satisfy the following condition: $L >> R_c$. Therefore, this method is usually applied for the case of a very large system size L or a very small R_c, as BCOY showed previously.[9] In the present work on PM melt chain simulations $L < 8R_c$, and hence the atom decomposition algorithm was found to be more efficient than the spatial domain decomposition method due to better load balancing.[25] For phantom chains, we assigned each processing node equal numbers of chains, since there are no interprocessor communications of forces and positions during simulations. For the melt chains, despite extensive interprocessor communications, our method yielded an overall efficiency better than 75% for up to 32 nodes. The SHAKE algorithm to constrain bond lengths using an iterative scheme requires extensive interprocessor communications if the atoms of one chain are distributed over different processors. Partitioning by a chain decomposition scheme can avoid this problem but will cause severe load imbalance for most expensive nonbonded force calculations. Therefore, the bond length constraint was not used in parallel computations, except for the phantom chain cases which require no interprocessor communications. A small time step of 0.5 fs was taken for parallel MD computations because of presence of flexible bonds and explicit hydrogen atoms while 1.0 fs was used for the SHAKE algorithm with bond length constraint. Usually, there are data passing errors in interprocessor communications. They are on the order of 10^{-8} for a single passing operation in this work with double precision data structure. These errors do not have any practical consequences for the MD trajectories since there is no error accumulation in the forces and

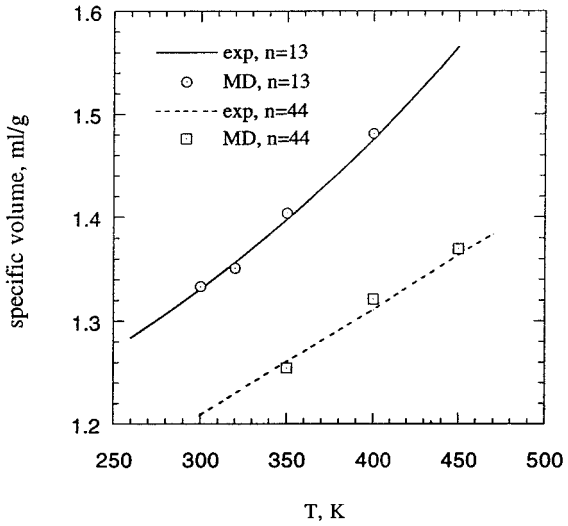

Figure 1. Temperature dependences of specific volume at 1 atm for polymethylene (C_nH_{2n+2}) melts with $n = 13$ and $n = 44$. Lines represent experiments,[26] and symbols are from simulations.

virials, because they are set to zero before every time step.

Results and Discussion

The previous work[16−18] based on *NVT* MD simulations with the same EA force field showed that simulated PM (C_nH_{2n+2}) melt systems of n =13 and 44 predicted many equilibrium and dynamic properties in good agreement with experiments. When sampled by *NPT* MD methods in this work, the simulated specific volume−temperature results are in good agreement with experiments,[26] as shown in Figure 1 for PM melts with n =13 and 44. (These are block averaged values over 400 ps trajectories at each temperature.) This agreement, taken together with the results of all the previous simulation work on equilibrium and dynamic properties of PM chains using the same EA force field, provides a strong support for the assumption that our simulation results of conformational properties of melt chains and phantom chains can be considered to be a good representation of real polymethylene chains.

Conformational Properties of Melt Chains and Various Phantom Chains. We calculated conformer populations, mean-square radii of gyration, and mean-square end-to-end distances as the averages of 2 ns trajectories from equilibrium MD runs and BD runs for melt chains and phantom chains of $C_{13}H_{28}$ and $C_{44}H_{90}$. In the present work, four types of phantom chains were studied, defined as follows: (1) 1,4 phantom chains including nonbonded interatomic interactions between atom pairs separated by up to three skeletal bonds; (2) 1,5 phantom chains including interactions for atom pairs separated by up to four skeletal bonds; (3) 1,6 phantom chains including interactions for atom pairs separated by up to five skeletal bonds; (4) all-atom phantom chains which consider all the atom pairs within a cutoff distance of 9 Å. The classical second-order RIS model is therefore a simplification of 1,5 phantom chains which approximates continuous torsional distributions by three discrete isomeric states (i.e., trans (t), gauche$^+$(g^+), and gauche$^-$ (g^-)) for each bond, while keeping the bond lengths and valence angles to be fixed.

Well-equilibrated conformational properties can be seen from the average torsional probability distribution

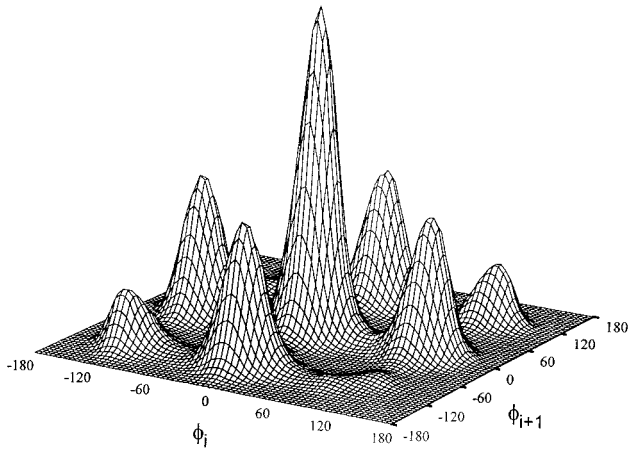

Figure 2. Conformational population contours for a pair of adjacent torsional angles (ϕ_i, ϕ_{i+1}) obtained from simulations of PM melts with $n = 44$ at 413 K.

for two consecutive C−C bonds. Plotted in Figure 2 is a two-dimensional density map for $C_{44}H_{90}$ at 413 K, as an example, with the trans state at $\phi = 0°$. Density peaks in Figure 2 are, from highest to lowest, in the order tt > tg$^\pm$ or g$^\pm$ t > g$^\pm$g$^\pm$ while g$^-$g$^+$ and g$^+$g$^-$ are much less populated than the others. An interesting splitting of the g$^+$g$^-$ or g$^-$g$^+$ state can be seen in Figure 2. This conformer population contour map is qualitatively similar to the energy contour map found for *n*-pentane,[4,11] except that the energy contour map tends to emphasize detailed features around high energy states such as the splitting of the g$^+$g$^-$ minimum. We now discuss the statistical results of interest to compare the conformational characteristics of melt chains and various phantom chains.

The averaged conformational properties are listed in Table 2 for $C_{44}H_{90}$ chains at 413 K. Trans conformer fractions, f(t), and pairwise conformer populations were calculated by conventional notation.[16] Also shown are the mean-squared end-to-end distances, $\langle r^2 \rangle$, and mean-squared radii of gyration, $\langle s^2 \rangle$. RMS errors in these statistics are less than 1% for conformer populations, < 5% for $\langle r^2 \rangle$, and < 2% for $\langle s^2 \rangle$. The values of trans conformer fraction, $\langle r^2 \rangle$ and $\langle s^2 \rangle$ of PM melts in Table 2 are basically the same as those reported in ref 17, other than the comment that the present results are considered to be statistically more reliable because they are based on longer trajectories.

The results in Table 2 show that all-atom phantom chains exhibit a considerable shrinkage of chain dimensions, consistent with previous results,[5−7] due to the fact that vacuum is a very poor solvent: i.e., the total excluded volume is negative at this temperature. As expected, 1,5 phantom chains are more extended than 1,4 phantom chains due to the second-order g$^\pm$g$^\mp$ repulsions, i.e., the well-known pentane effect. As the 1,6 intramolecular interactions are added, the local conformer fractions remain the same within the ±1% statistical uncertainty. The overall chain dimension appears to shrink by ca. 2−4%, but this is still within the statistical uncertainty. Hence, according to the realistic EA force field, the short-range intramolecular interactions which determine the unperturbed PM chain characteristics can be restricted to 1,4 and 1,5 interactions, in agreement with the rationale of the second-order RIS model.[2−4,10,11]

Previously, SBRM found a considerable decrease (by ca. 7%) in $\langle r^2 \rangle$ and $\langle s^2 \rangle$ for 1,6 phantom chains as compared with those of 1,5 phantom chains.[5] Our

Table 2. Conformer Fractions, *f*, and Chain Dimensions, $\langle r^2 \rangle$ and $\langle s^2 \rangle$, of $C_{44}H_{90}$ Chains in Melts and in Various Phantom Chains at 413 K

properties	melt chains	1,4 phantom	1,5 phantom	1,6 phantom	all-atom phantom
f(t)	0.60	0.47	0.59	0.58	0.55
f(tt)	0.34	0.22	0.34	0.33	0.30
f(tg)	0.53	0.48	0.52	0.53	0.51
$f(g^{\pm}g^{\pm})$	0.11	0.15	0.11	0.12	0.15
$f(g^{\pm}g^{\mp})$	0.02	0.14	0.03	0.03	0.03
$\langle r^2 \rangle$, Å^2	716	393	725	712	423
$\langle s^2 \rangle$, Å^2	95	52	96	92	57

finding differs from theirs; this difference may reflect stronger interatomic attractions between united atom centers than those between carbon atoms in the EA model. They also concluded that 1,6 phantom chains correspond to unperturbed PM chains. This was based on their implicit solvent model calculations which scale the attractive part of the Lennard−Jones interactions by a factor β, between the two atoms separated by a distance r_{ij}:

$$u(r) \propto \left[\left(\frac{\delta}{r_{ij}}\right)^{12} - \beta\left(\frac{\delta}{r_{ij}}\right)^{6}\right] \qquad (1)$$

They concluded that a value of β close to 0.55 at 400 K led to the ideal, unperturbed chains showing $\langle r^2 \rangle$ to be linearly proportional to the number of bonds and that the value of $\langle r^2 \rangle$ for such an ideal chain corresponded to that of 1,6 phantom chains, calculated without any scaling of the attractive interactions. However, the maximum chain length investigated by SBRM was n =150. In a very recent work, DLR extended the chain length to n =2000 using the same united atom force field in order to get a better estimate of excluded volume effects and found that the ideal PM chain, devoid of any excluded volume effects, is obtained with the attractive interaction scaling factor $\beta = 0.505$.[6] Such an unperturbed chain is slightly more extended than that with $\beta = 0.55$, and its properties are closer to 1,5 phantom chains than those of 1,6 phantom chains, according to the results of SBRM.[5] Therefore, the contraction of phantom chains upon inclusion of additional intramolecular interactions beyond the 1,5 interactions, as shown by SBRM[5] and BQPB,[7] can be attributed to the long-range (negative) excluded volume interactions.

Though we have not carried out corresponding implicit solvent model calculations using the EA force field, based on the UA model results of SBRM[5] and DLR,[6] it is most unlikely that we need to include any intramolecular interactions beyond 1,6 interactions in order to determine the characteristics of real unperturbed PM chains. In this regard, since our results based on a realistic EA model show practically no difference between the conformational properties of 1,5 phantom chains and those of 1,6 phantom chains, we can conclude that the conformational characteristics of unperturbed PM chains can be accurately represented by those of 1,5 phantom chains.

Furthermore, the conformational properties of $C_{44}H_{90}$ melt chains listed in Table 2 are found to be identical to those of 1,5 phantom chains, within ±1%, for all properties considered. Compared with those of 1,6 phantom chains, the melt chains appear to expand, by about 3% in $\langle s^2 \rangle$. Hence, even if 1,6 phantom chains are closer to unperturbed chains, the conformational characteristics of melt chains are considered to be identical to those of unperturbed chains within the statistical accuracy, ±2% in $\langle s^2 \rangle$, of our simulations.

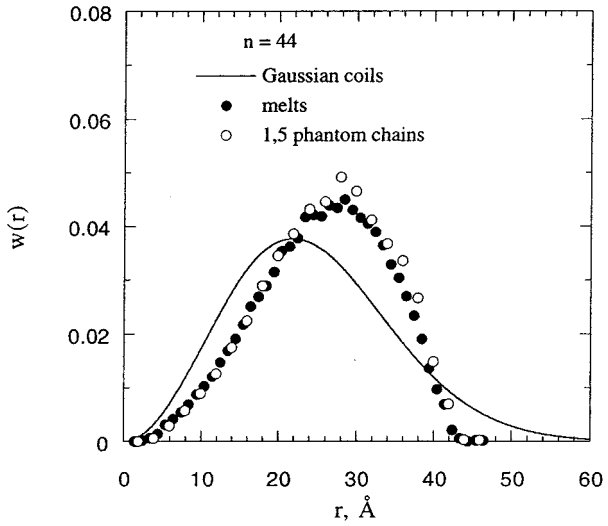

Figure 3. End-to-end distance distribution functions, $w(r)$, obtained from simulations of $C_{44}H_{90}$ chains in melts and 1,5 phantom chains at 413 K, compared with the Gaussian distribution.

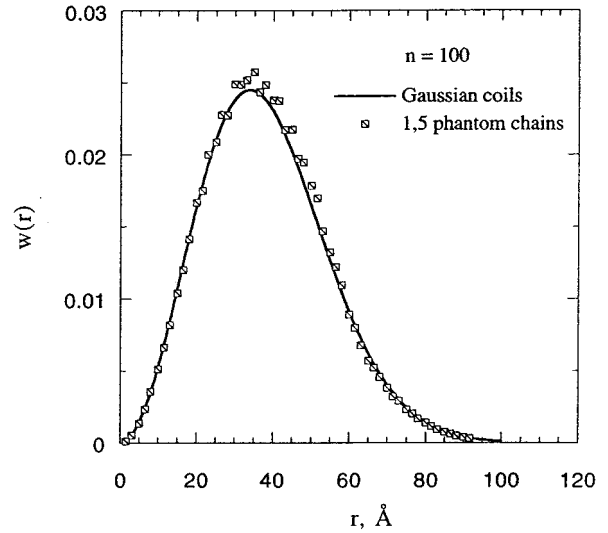

Figure 4. End-to-end distance functions, $w(r)$, obtained from simulations of 1,5 phantom chains of $C_{100}H_{202}$ at 413 K, compared with the Gaussian distribution.

Distribution of End-to-End Chain Distances. We calculated the distribution functions, $w(r)$, of end-to-end distances and, $w(s)$, of radii of gyration for melt chains and various phantom chains of $C_{44}H_{90}$. Figure 3 presents the results for the melt and 1,5 phantom chains for $C_{44}H_{90}$, and Figure 4 shows the 1,5 phantom chain results for $C_{100}H_{202}$. Also shown in these figures are the Gaussian distribution functions, calculated by

$$w(r) = 4\pi r^2 \left(\frac{3}{2\pi\langle r^2 \rangle}\right)^{3/2} \exp\left(-\frac{3r^2}{2\langle r^2 \rangle}\right) \qquad (2)$$

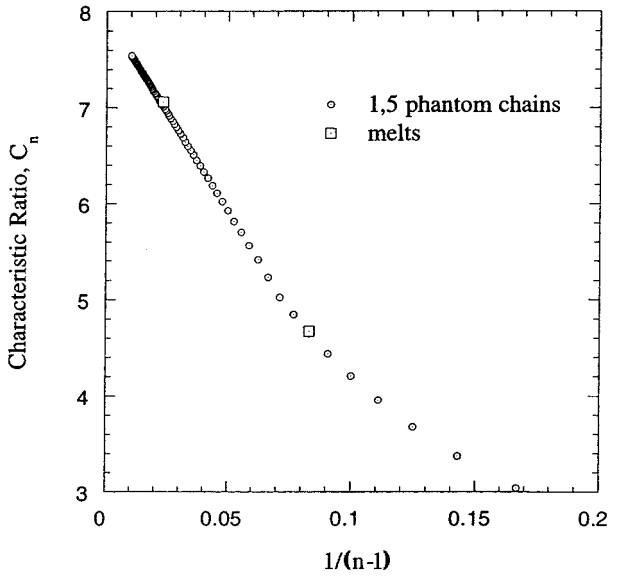

Figure 5. Characteristic ratio, C_n, for PM segments comprising n methylene units within 1,5 phantom chains of $C_{100}H_{202}$, together with the values for PM melt chains with $n = 13$ and 44, all at 413 K.

where the mean-square end-to-end distance $\langle r^2 \rangle$ is taken from the simulation values.

In Figure 3, the results for melt chains and 1,5 phantom chains essentially fall on the same curve, further confirming that the melt chain statistics are identical to those of the 1,5 phantom chains and hence to those of the unperturbed chains. Moreover, this distribution of end-to-end distances for $C_{44}H_{90}$ shows a significant deviation from the Gaussian function. For $C_{100}H_{202}$ chains the 1,5 phantom chain results can be considered to correspond to those of unperturbed chains as well as those of melt chains, as discussed above. The general feature of the simulation results in Figure 4 is well fitted to the Gaussian distribution, but a closer look shows a slight deviation from the Gaussian distribution, in both the position and the height of the maximum in $w(r)$. Hence, it is clear that PM chains of $n \leq 100$ are not fully Gaussian, as was suggested previously by Monte Carlo simulations of RIS model chains.[19]

Characteristic Ratio of PM Chains. We calculated the characteristic ratios, C_n ($=\langle r^2 \rangle/(n-1)l^2$), for melt chains of C_nH_{2n+2} with $n = 13$ and 44, and also determined the corresponding value C_n for the chain segments comprised of n monomer units within 1,5 phantom chains of $C_{100}H_{202}$, defined by

$$C_n = \frac{\langle r_n^2 \rangle}{(n-1)\,l^2} = \frac{1}{(100-n+1)\,(n-1)l^2} \sum_{i=1}^{100-n+1} \langle r_{i,i+n-1}^2 \rangle \quad (3)$$

where $r_{i,j}$ is the distance between the ith and jth carbon atoms along the chain. Both sets of results are shown in Figure 5, denoted by squares and circles, respectively. The results for melt chains and segments of 1,5 phantom chains are indistinguishable. The values of C_n varies almost linearly with $1/n$ for $1/n < 0.05$, and extrapolation to the high molecular weight limit yields a value of $C_\infty \approx 7.9$ at 413 K.

Previously, DLR found a value of $C_\infty = 7.9 \pm 0.2$ at 400 K for unperturbed PM chains from a careful simulation study of implicit solvent systems.[6] They noted that this value is considerably greater than the generally accepted experimental value of 6.8 for polyethylene at 400 K but attributed the discrepancy to a deficiency in their UA force field parameters. Since our work, based on well-calibrated EA force field parameters, shows the same deviation from previous experimental values, the origin of this discrepancy needs to be considered more carefully.

The experimental characteristic ratios for polyethylenes were determined mainly from the intrinsic viscosity data in Θ solvents. Chiang first reported a value of 6.7 at 435 K,[27] followed by Nakajima, Hamada, and Hayashi, who reported values of 6.8 at 437 K, 7.0 at 415 K, and 7.1 at 400 K,[28] applying the Flory−Fox equation with a universal constant of $\Phi = 2.5 \times 10^{21}$. Even though the samples were carefully fractionated by precipitation, they should be considered to be relatively polydisperse. Recently, using nearly monodisperse polyethylene samples with two ethyl branches per 100 backbone carbons, Horton et al. reported a value of 7.8 ± 0.4 for melt chains at 413 K from small angle neutron scattering (SANS) experiments.[20] Most recently, Fetters et al. investigated chain dimensions in the melt for polyethylene samples with varying ethyl branch contents by SANS experiments.[29] Upon extrapolation to zero branch content, their results yield a characteristic ratio of ca. 7.5 for polyethylene at 413 K. Therefore, the recent SANS experiments for the melt samples definitely exhibit characteristic ratios considerably greater than those derived from intrinsic viscosity data. The problem with the earlier studies is most likely due to the use of polydisperse samples and the uncertainty of adopting a value of $\Phi = 2.5 \times 10^{21}$ for such polydisperse samples.[30] On the other hand, the temperature coefficient of chain dimensions, $d \ln\langle r^2 \rangle / dT = -(1.06-1.25) \times 10^{-3}$/K, from SANS experiments for the melt chains[31] is in complete agreement with intrinsic viscosity results of $-(1.1-1.2) \times 10^{-3}$/K derived from experimental data in different Θ solvents.

Comparison with Rotational Isomeric State Model Calculations. In the present work, we used the established second-order RIS model to estimate the characteristic ratio and its temperature coefficient using appropriate geometric and energetic parameters from the EA force field. RIS model parameters obtained from the EA force field used in this work with the bond length (l) fixed at 1.53 Å are 112° for the valence angle (θ), 113.4° for the torsion angle (ϕ_g) at gauche states, 0.48 kcal/mol for the first-order gauche energy (E_σ), and 2.1 kcal/mol for the second-order g^+g^- energy (E_ω). This RIS model yields a characteristic ratio C_∞ of 7.8 and a temperature coefficient of -1.14×10^{-3}/K at 413 K. This is consistent with the previous RIS calculations that show a characteristic ratio of 7.9 for $\phi_g = 112.5°$, while keeping the other parameters the same as in the previous model (i.e., $l = 1.53$ Å, $\theta = 112°$, $E_\sigma = 0.5$ kcal/mol, and $E_\omega = 2.0$ kcal/mol).[4,11] The gauche energy, E_σ, is found to be in agreement with the estimates from the spectroscopic data[32] as well as high-level quantum chemical calculations.[18,33] We also computed the geometry and energy of the $g^\pm g^\mp$ minimum of n-pentane using the 6-311G** basis set at the MP2 level electron correlation and found its energy to be 2.7 kcal/mol above the tt minimum, in good agreement with the RIS value of 3.0 kcal/mol. The geometric parameters for the bond lengths and valence angles are well-known from experiments. Therefore, the only uncertainty exists for the

gauche torsional angles. The choice of $\phi_g = 120°$ in the previous RIS model, despite the apparent value of 112.5° from the energy contours, was made mainly to match the apparent experimental characteristic ratio of 6.8. In this regard, both recent SANS experiments and our EA model simulations show that the RIS model with a realistic value of $\phi_g = 113°$ will be a better representation of polymethylene chains, yielding a characteristic ratio of 7.8 and its temperature coefficient of -1.1×10^{-3}/K at 413 K in agreement with experiments and simulations.

Summary

Molecular simulations with a well-calibrated EA force field have been applied to study the conformational characteristics of PM chains in melts and in various phantom chains. No discernible differences are found between the characteristics of 1,5 phantom chains and 1,6 phantom chains, while a significant shrinkage is seen for the all-atom phantom chains. This result, taken together with recent work by SBRM[5] and DLR,[6] who applied the implicit solvent model to determine the Θ-solution characteristics, clearly demonstrates that the short-range interactions defining unperturbed PM chains are fully accounted for by 1,5 phantom chains, in agreement with the previous proposition of second-order RIS models. Moreover, the characteristics of PM chains in melts are shown to be identical to those of 1,5 phantom chains, i.e., unperturbed chains, in conformer populations, chain dimensions, and distributions of end-to-end distances. The distribution of end-to-end distances shows a significant deviation from the Gaussian function for $C_{44}H_{90}$ chains and a slight but still noticeable deviation for $C_{100}H_{202}$, indicating that one should be careful in representing PM chain sequences of $n \leq 100$ by Gaussian models. The characteristic ratio C_∞ for high molecular weight polyethylenes is found to be ca. 7.9 at 413 K according to our EA molecular simulations. This value is considerably greater than the generally accepted experimental value, 6.8, derived from the intrinsic viscosity data for relatively polydisperse samples, but is corroborated by the recent SANS result, $C_\infty = 7.8 \pm 0.4$, obtained for melt chains of nearly monodisperse samples. This new value of characteristic ratio can be represented readily by the established RIS model by simply using a more realistic value for the gauche torsional angle, $\phi_g = 113°$, instead of 120° as used previously. This revised RIS model yields $C_\infty = 7.8$ and its temperature coefficient, $d(\ln\langle r^2\rangle_0)/dT = -1.1 \times 10^{-3}$/K, both in good agreement with recent SANS experiments.

Concluding Remarks

The representation of unperturbed PM chains by the simulated phantom chains as well as by the implicit solvent model calculations is critically dependent on the approximation that polymer segment−solvent interactions (attractions) remain the same regardless of local chain conformations. Since Flory's proposition of identifying the melt chain characteristics with those of unperturbed chains is built on this same assumption of no correlations between the intramolecular conformations and intermolecular attractions, our finding that melt chains are practically identical to 1,5 phantom chains may indeed be regarded as validating such an assumption for PM chains. In this regard, it should be noted that such an assumption is not always valid. For example, for polystyrene it was suggested that in the trans-trans conformation within meso diad, the adjacent pendent side groups within the polymer chain are very close to each other, thereby limiting close van der Waals contacts with solvents, which are fully allowed for other conformations.[34] In such a case, phantom chains cannot rigorously represent unperturbed chains or melt chains,[35] nor can an implicit solvent model be used to determine the unperturbed chain characteristics.

Moreover, when there are correlations between the short range intramolecular conformations and the intermolecular attractions, the chain conformations in the melt will be the same as those in Θ solutions only if the nature of such correlations in the melts are practically the same as those in Θ solvents. In this regard, it was shown very recently by both molecular simulations and SANS experiments that the conformational characteristics of poly(oxyethylene) chains in the melt differ significantly from those in Θ solutions owing to the presence of significant dipole-dipole and CH···O attractions between the segments of neighboring chains which vary strongly with local conformations of poly(oxyethylene) chains.[36] The model molecule, 1,2-dimethoxyethane, is also seen to assume different conformations in the liquid state from those in the gas phase by both experiments[37] and simulations[38] for the same reason. Certainly this line of inquiry deserves much more attention both experimentally and theoretically, since the consequences of such condensed phase effects are expected to be very important for understanding the properties of various bulk polymeric materials.

Acknowledgment. We wish to sincerely thank Dr. L. J. Fetters for discussing the SANS data for melt chains of polyethylenes and also making available to us the manuscript on PE copolymers, and we also acknowledge the help of Dr. G. D. Smith in providing the initial $C_{44}H_{90}$ systems. J. H. is very grateful for the financial assistance of the National Research Council postdoctoral associateship program through the NASA Ames Research Center.

References and Notes

(1) Flory, P. J. *J. Chem. Phys.* **1949**, *17*, 303; *Proc. R. Soc. London, A* **1956**, *234*, 6; *Pure Appl. Chem.* **1984**, *56*, 305.
(2) Volkenstein, M. V. *Configurational Statistics of Polymeric Chains*; translated from the Russian ed., 1959, by S. N. and M. J. Timasheff; Interscience: New York, 1963.
(3) Birstein, T. M.; Ptitsyn, O. B. *Conformations of Macromolecules;* translated from the Russian ed., 1964, by S. N. and M. J. Timasheff; Interscience: New York, 1966.
(4) Flory, P. J. *Statistical Mechanics of Chain Molecules*; Interscience: New York, 1969.
(5) Sariban, A.; Brickmann, J.; van Ruiten, J.; Meier, R. J. *Macromolecules* **1992**, *25*, 5950.
(6) Destrée, M.; Lyulin, A.; Ryekaert, J.-P. *Macromolecules* **1996**, *29*, 1721.
(7) Baschnagel, J.; Qin, K.; Paul, W.; Binder, K. *Macromolecules* **1992**, *25*, 3117.
(8) Pant, P. V. K.; Theodorou, D. N. *Macromolecules* **1995**, *28*, 7224.
(9) Brown, D.; Clarke, J. H. R.; Okuda, M.; Yamazaki, T. *J. Chem. Phys.* **1994**, *100*, 1684; *J. Chem. Phys.* **1996**, *104*, 2078.
(10) Lifson, S. *J. Chem. Phys.* **1959**, *30*, 964. Nagai, K. *J. Chem. Phys.* **1959**, *31*, 1169. Hoeve, C. A. J. *J. Chem. Phys.* **1960**, *32*, 888.
(11) Abe, A.; Jernigan, R. L.; Flory, P. J. *J. Am. Chem. Soc.* **1966**, *88*, 631.
(12) Zirkel, A.; Richter, D.; Fetters, L.; Schneider, D.; Graciano, V.; Hadjichristidis *Macromolecules* **1995**, *28*, 5262.
(13) Toxvaerd, S. *J. Chem. Phys.* **1990**, *93*, 4290.
(14) Yoon, D. Y.; Smith, G. D.; Matsuda, T. *J. Chem. Phys.* **1993**, *98*, 10037.

(15) Sorensen, R. A.; Liau, W. B.; Kesner, L.; Boyd, R. H. *Macromolecules* **1988**, *21*, 200.
(16) Smith, G. D.; Yoon, D. Y. *J. Chem. Phys.* **1994**, *100*, 649.
(17) Smith, G. D.; Yoon, D. Y.; Zhu, W.; Ediger, M. D. *Macromolecules* **1994**, *27*, 5563.
(18) Smith, G. D.; Yoon, D. Y.; Jaffe, R. L. *Macromolecules* **1995**, *28*, 5897.
(19) Yoon, D. Y.; Flory, P. J. *J. Chem. Phys.* **1974**, *61*, 5366.
(20) Horton, J. C.; Squires, G. L.; Boothryod, A. T.; Fetters, L. J.; Rennie, A. R.; Glinka, C. J.; Robinson, R. A. *Macromolecules* **1989**, *22*, 681.
(21) Nosé, S. *J. Chem. Phys.* **1984**, *81*, 512.
(22) Winkler, R. G.; Matsuda, T.; Yoon, D. Y. *J. Chem. Phys.* **1993**, *98*, 729.
(23) Helfand, E.; Wasserman, Z. R.; Weber, T. A. *Macromolecules* **1980**, *13*, 526.
(24) Adolf, D.; Ediger, M. D. *Macromolecules* **1991**, *24*, 5834.
(25) Han, J.; Jaffe, R. L.; Yoon, D. Y. Parallel Molecular Dynamics Simulation of Polymers: Atom Decomposition Algorithm. Manuscript in preparation.
(26) Timmermans, J. *Physico-Chemical Constants of Pure Organic Compounds,* Elsevier Publishing: New York, 1965.
(27) Chiang, R. *J. Phys. Chem.* **1965**, *69*, 1645; *J. Phys. Chem.* **1966**, *70*, 2348.
(28) Nakajima, A.; Hamada, F; Hayashi, S. *J. Polym. Sci., Part C* **1966**, *15*, 285.
(29) Fetters, L. J.; Graessley, W. W.; Krishnamoorti, R.; Lohse, D. J. *Macromolecules* **1997**, *30*, 4973.
(30) Newman, S.; Krigbaum, W. R.; Laugier, C.; Flory, P. J. *J. Polym. Sci.* **1954**, *XIV*, 451.
(31) Boothroyd, A. R.; Rennie, A. R.; Boothroyd, C. B. *Europhys. Lett.* **1991**, *15*, 715.
(32) Scherer, J.; Snyder, R. G. *J. Chem. Phys.* **1980**, *72*, 5798.
(33) Smith, G. D.; Jaffe, R. L. *J. Phys. Chem.* **1996**, *100*, 18718.
(34) Yoon, D. Y.; Sundararajan, P. R.; Flory, P. J. *Macromolecules* **1975**, *8*, 776.
(35) Han, J.; Jaffe, R. L.; Yoon, D. Y. Manuscript in preparation.
(36) Smith, G. D.; Yoon, D. Y.; Jaffe, R. L.; Colby, R. H.; Krishnamoorti, R.; Fetters, L. J. *Macromolecules* **1996**, *29*, 3462.
(37) Yoshida, H.; Kaneko, I.; Matsuura, H.; Ogawa, Y.; Tasumi, M. *Chem. Phys. Lett.* **1992**, *196*, 601.
(38) Smith, G. D.; Jaffe, R. L.; Yoon, D. Y. *J. Am. Chem. Soc.* **1995**, *117*, 530.

MA961772B